Lifetime Seismic Risk Assessment of Coastal Highway Bridges under Corrosion, Scour and Liquefaction Effects

Xiaowei Wang
Associate Professor, Dept. of Bridge Engineering, Tongji University, Shanghai, China

Bo Xu
Ph.D. Student, Dept. of Civil and Environ. Engineering, Case Western Reserve University, Cleveland, USA

Yue Li
Professor, Dept. of Civil and Environ. Engineering, Case Western Reserve University, Cleveland, USA

ABSTRACT: Coastal highway bridges, particularly those with reinforced concrete members, are susceptible to chloride-induced corrosion in their lifetime due to the aggressive coastal environment. Such an adverse environment has also witnessed the susceptibility and vulnerability of bridges to multi-hazard events during their service life; such events include, but are not limited to, scour and earthquake-induced liquefaction. This study carries out a risk-informed assessment to understand the influence of corrosion (represented by service time) and scour (represented by scour depth) on the seismic behavior of coastal bridges in liquefiable ground. To this end, a typical highway bridge is adopted as a testbed structure, which is simulated using OpenSees with a mul-ti-dimensionally soil-structure modeling technique. Through probabilistic seismic demand analyses and ca-pacity modeling, fragility curves are generated for different scenarios of corrosion, scour, and liquefaction ef-fects. Together with probabilistic seismic hazard analyses, time-dependent seismic risk of highway bridges can be obtained to better understand the roles of these effects in the lifetime performance assessment. It is found that the seismic risk of bridge pile foundation apparently increases with the increase of service time as well as scour depth. In particular, the role of scour depth become significant during service time from 40 to 60 years. This pilot study can facilitate risk-informed decision-on life-cycle management of coastal highway bridges under the ever-changing multi-hazard threats.

Coastal highway bridges always serve as paramount components in transportation networks of coastal regions. Such regions are commonly existed for years and are densely populated with prospect economic development. Long-standing transportation infrastructure occupies a major portion of a nation's assets. On the other hand, the aging highway bridges have attracted intensive attention in both industrial and academic communities. A noticeable issue is the steel corrosion and associated concrete deterioration, as shown in Figure 1(a). For this reason, extensive studies have been conducted to assess the effect of service time on the behavior of bridges under natural hazards such as earthquakes (Ghosh & Padgett, 2010). Existing studies mainly focus on the seismic behavior of bridge columns and bearings under corrosive environments, while rare studies assess bridge pile foundations. This problem becomes more important when pile-foundation-related natural hazards are involved, such as scour (Figure 1(b)) and liquefaction under earthquakes (Wang et al., 2019). However, there is a noted knowledge gap in the understanding of corrosion and scour effects on seismic risk of coastal highway bridges in liquefiable soils.

To fill in the abovementioned gap, this study assessed the lifetime seismic risk of coastal highway bridges under corrosion, scour, and liquefaction scenarios. Well-validated coupled soil-bridge finite element (FE) models are adopted to conduct massive nonlinear dynamic

analyses for seismic fragility and risk assessment. This paper begins with an introduction of the adopted method for seismic risk estimates, followed by the detailing of FE modeling. Finally, seismic fragility and risk assessment results are presented and discussed.

(a) (b)

Figure 1. Illustration of study object: (a) typical corrosion issues for bridges (photo by the authors), and (b) a typical highway bridge in a scour scenario (by courtesy of Professor Yi-Ching Lin)

1. SEISMIC RISK ASSESSMENT METHOD

In structural engineering, seismic risk is often defined as the annual probability (λ) of the seismic demand (D) exceeding the prescribed limit state (C). The seismic risk can be quantified by convolving the fragility (P) with the hazard (H) curves in terms of an optimal seismic intensity measure (IM), as expressed in Equation (1):

$$\lambda = \int P[C < D|IM] \cdot |dH(IM)| \qquad (1)$$

where $P[C < D|IM]$ is the seismic fragility, which can be calculated using probabilistic seismic demand analyses (e.g., the adopted *Cloud* method (Cornell et al., 2002)), together with prescribed structural limit states, as expressed as a lognormal cumulative distribution function (Φ):

$$P[C < D|IM] = \Phi\left[\frac{\ln(a \cdot IM^b/C)}{\sqrt{\beta_{D|IM}^2 + \beta_C^2}}\right] \qquad (2)$$

where a and b are regression coefficients for the estimate of seismic demand in an assumed power-law form (i.e., $D = a \cdot IM^b$). $\beta_{D|IM}$ and β_C represent dispersions of the demand and capacity, respectively. $H(IM)$ in Equation (1) is the seismic hazard that describes the annual probability of earthquake excitation intensity exceeding IM, which can be calculated as:

$$H(IM) = k_0 \cdot IM^{-k} \qquad (3)$$

where k_0 and k are constants that are dependent on site conditions. Substituting Equations (2) and (3) into Equation (1) leads to the following equation for the seismic risk estimate (Han et al., 2014):

$$\lambda = H\left[(C/a)^{1/b}\right] \cdot \exp\left[\frac{k^2}{2b^2}(\beta_{D|IM}^2 + \beta_C^2)\right] \qquad (4)$$

2. FINITE ELEMENT MODELING

2.1. Coupled soil-bridge modeling

The study object is typical multi-span coastal RC highway bridges with each bent supported by a single column and a pile-group foundation under a corrosive environment against scour and earthquake-induced liquefaction hazards. Each bent of such bridges has fairly close stiffness and similar soil profile conditions. For this reason, the multi-span bridge is simplified as a single column with a lumped mass to represent the deck and supported by a pile-group embedded into liquefiable soils with scour potential.

OpenSees is adopted to mimic such a complex coupled soil-bridge system using a multi-dimensional finite element (FE) modeling technique that can balance the simulation accuracy and computational costs (Wang et al., 2017). Figure 2 briefly illustrates the FE model. Before corrosion, the column and piles have longitudinal reinforcement ratios of 1.5% and 1.0%, respectively, using 28mm rebars, while the stirrups are represented by 20mm rebars with an interval of 100m. More FE modeling details and associated model validation refer to the authors' former study (Wang et al., 2019). It is worth noting that the hydrodynamic effect can be generally ignored for probabilistic seismic demand analyses of coastal highway bridges in liquefiable sites (Wang et al., 2020b), thereby this effect is not considered in the present study. Three scour scenarios represented by scour depths of 0m (intact), 3m and 6m are considered. Regarding the engineering demand parameter, only the

maximum pile curvature is assessed for conciseness, as piles are the vulnerable component of a bridge in liquefied and scoured sites (Wang et al., 2020a).

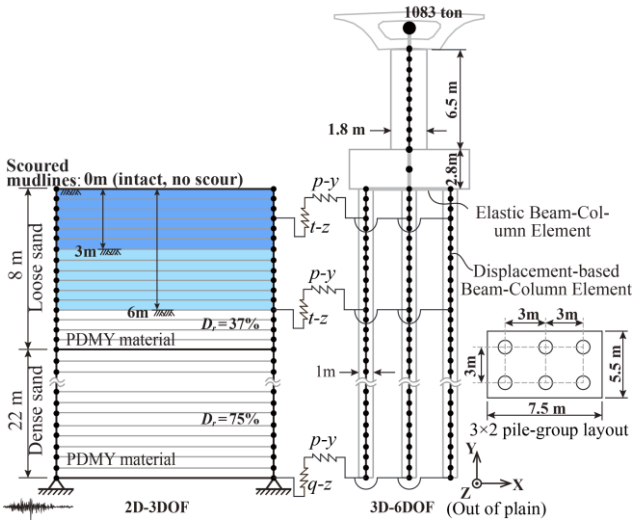

Figure 2. Schematic illustration of FE modeling of the coupled soil-bridge model

2.2. RC material constitutive models and section limit states accounting for corrosion effect

Effects of corrosion on RC materials are mainly reflected by the degradation of reinforcing steel (both rebar and stirrup) and concrete cover strengths. The confined concrete core is affected accordingly. The material constitutive laws for intact and corroded rebars and concrete are schematically illustrated in Figure 3.

More specifically, the residual strength of corroded reinforcing steels can be estimated by Equation (5) (Du et al., 2005):

$$f_{y,cor} = \left(1.0 - \beta_y Q_{corr}\right) f_y \tag{5}$$

where Q_{corr} is corrosion percentage of cross sectional area of rebars (Ghosh & Padgett, 2010); $f_{y,cor}$ and f_y are yield strengths of corroded and non-corroded (i.e., intact) steels, respectively; β_y is the attenuation coefficient, set as 0.0124 (Lee & Cho, 2009).

On the other hand, due to the corrosive expansion of steels, the compressive strength of surrounding concrete decreases, as represented by Equation (6) (Coronelli & Gambarova, 2004):

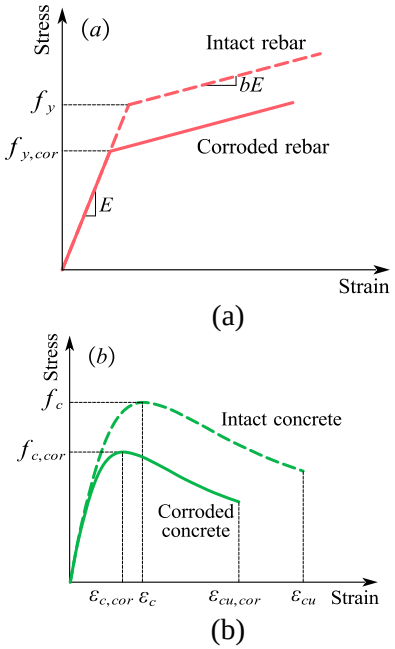

Figure 3. Constitutive laws for intact and corroded materials: (a) steel reinforcement and (b) concrete.

$$f_{c,cor} = \frac{f_c}{1 + K\dfrac{\varepsilon_1}{\varepsilon_{co}}} \tag{6}$$

where $f_{c,cor}$ and f_c are the compressive strength of corroded and intact concrete, respectively; K is the coefficient related to bar roughness and diameter. K = 0.1 can be adopted for medium-diameter ribbed bars (Capé, 1999); ε_{co} refers to the strain at the concrete peak compressive stress, while ε_1 is the average tensile strain in the cracked concrete, as:

$$\varepsilon_1 = n_{bars} 2\pi (v_{rs} - 1) X / b_0 \tag{7}$$

where b_0 is section width in the intact state; n_{bars} is the number of rebars; X is the corrosion depth; v_{rs} is the ratio of volumetric expansion of the oxides with respect to the intact state, which can be taken as 2.0 (Molina et al., 1993). In addition to the intact state (represented as 0 year), this study considers four corroded scenarios in terms of service time, i.e., 20, 40, 60, and 80 years. Since the corrosion process, as well as the RC material constitutive models, involve uncertainties, critical parameters are treated as random variables according to their uncertainty models, as listed in Table 1. 40 samples of these parameters are generated using the Latin hypercube sampling

technique for the scenario of 0 year, while the corroded scenarios are calculated according to Equations (5) to (7). Note that the number of 40 for the samples is determined according to the adopted 40 ground motions described later. Figure 4 shows strength versus service time relationships of the concrete and steel reinforcement. It can be seen that the service time strongly affects the steel and concrete cover strengths, i.e., a service time of 40 years leads to almost 50% degradation of stirrup strength, while for concrete cover, this level of degradation only needs 20 years.

Table 1. Statistical information on random variables related to corrosion process.

Variable	Distribution	Mean	COV*	Source
Diffusion coefficient, D_c (cm^2/s)	Lognormal	2.0E-8	0.1	(Ghosh & Padgett, 2010)
Surface chloride concentration, C_0 (kg/m^3)	Lognormal	3.5	0.5	(Stewart & Rosowsky, 1998)
Critical chloride concentration, C_r (kg/m^3)	Uniform	0.9	0.19	(Vu & Stewart, 2000)
Corrosion rate, r (mm^2/year)	Lognormal	0.127	0.3	(Ghosh & Padgett, 2010)

* Coefficient of variance

To quantify the limit state (LS) of the intact and corroded RC pile sections, moment-curvature analyses are conducted for each scenario. For conciseness, this study considers two LSs, namely slight and moderate LSs, denoted as LS_1 and LS_2, both in terms of section curvature. More specifically, LS_1 indicates the first-yield state of steel rebar, while LS_2 refers to the state when the concrete cover reaches its ultimate strain. Figure 3 shows the obtained LSs versus service time. Note that two vertical axes are used to demonstrate the decreasing tendency of curvature at LS_1, which is much smaller than that at LS_2. It is seen that the curvature at LS_1 gradually decreases (linearly on average) with respect to the service time, while that at LS_2 drops mostly in the first 20 years.

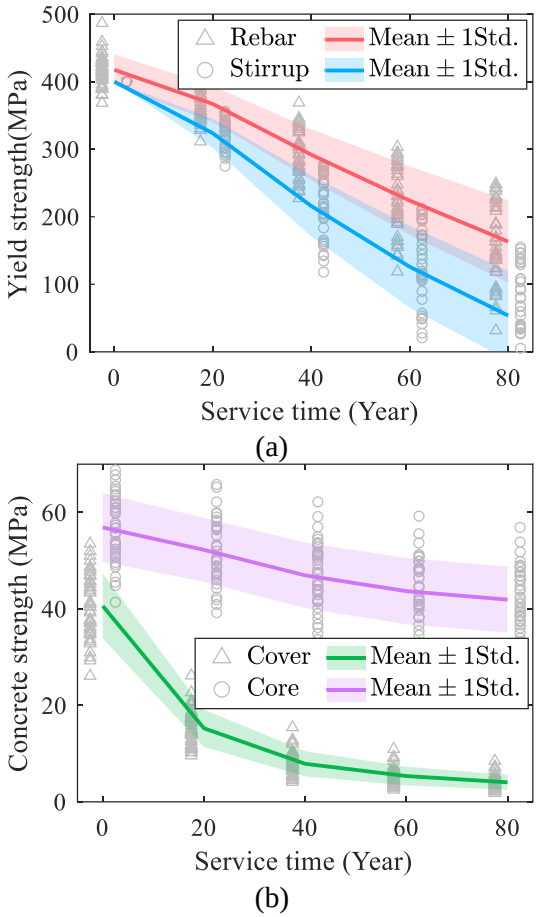

Figure 4. Changes of material strength with respect to service time: (a) steel reinforcement and (b) concrete.

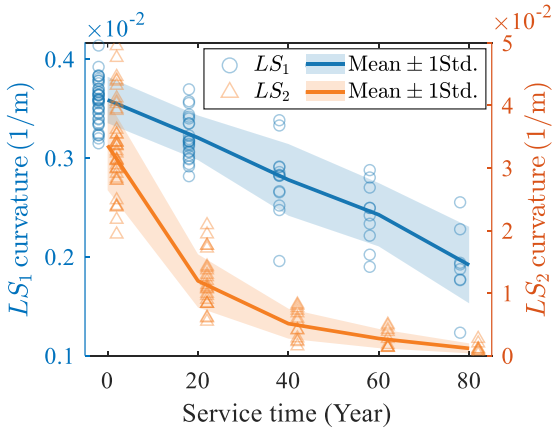

Figure 5. Limit states of pile sections with respect to service time (LS_1 indicates the first-yield state of steel rebar, while LS_2 refers to the state when the concrete cover reaches its ultimate strain.).

2.3. Adopted ground motions and hazard curve

40 non-pulse-like real ground motions for rock sites, which were selected by Baker et al. (2011) as a standardized set of ground motions for seismic analysis of transportation infrastructure in California, are adopted in this study for each scenario with different scour depths and service time. In light of Gehl et al. (2015), 40 dynamic analyses are deemed generally sufficient for deriving a reliable fragility curve using the *Cloud* method. In total, 40×3 (scour scenarios) ×5 (corrosion scenarios) = 600 nonlinear dynamic analyses are run in this study. Note that ground motions are input at the base of the soil column, which is supposed to lie on a very firm stratum on top of the bedrock. Soil surface acceleration time history responses are recorded to calculate the selected IM in this study, i.e., the spectral acceleration at 2.0s ($S_{a\text{-}20}$), which has been identified as an optimal IM for probabilistic seismic demand modeling of bridges in liquefiable ground (Wang et al., 2018).

In line with the adopted ground motions, a seismic hazard curve is fitted for the Los Angeles, California site that has an average shear velocity of 760 m/s, i.e., the boundary of site class B and C. More specifically, annual probabilities of exceedance at specific $S_{a\text{-}20}$ values are calculated using the Conterminous U.S. 2014 Model (version 4.2.0) (Petersen et al., 2015). Accordingly, the constants k_0 and k in Equation (3) are obtained as shown in Figure 6.

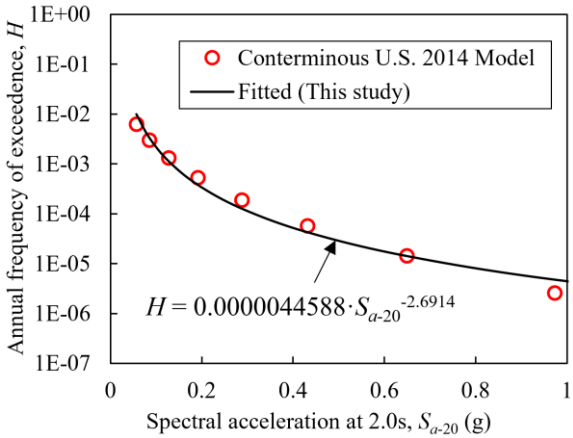

Figure 6. Seismic hazard curve for Los Angeles, California.

3. RESULTS AND DISCUSSIONS

3.1. Seismic fragility of pile foundation

Figure 7 indicatively shows pile fragility curves at two different limit states for two different scour scenarios. It is clear that the seismic damage probabilities increase with the increasing service time, regardless of scour depths and limit states, indicating that an aging pile-group foundation would become more and more vulnerable across its service life if no retrofit measures are applied. This phenomenon is a cause of the decreasing curvature capacities at LS_1 and LS_2 due to corrosion (see Figure 5), together with the increasing pile demands due to increased soil-pile kinematic interaction, although not shown for conciseness.

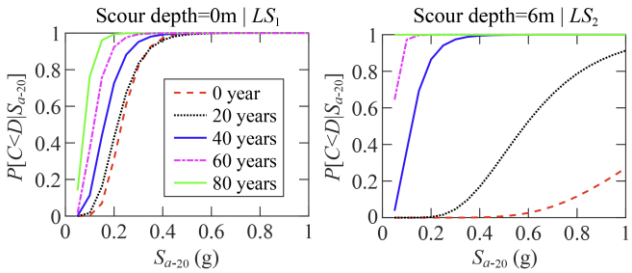

Figure 7. Representative fragility curves of piles at different limit states for different scour scenarios: (a) scour depth of 0m at LS_1, and (b) scour depth of 6m at LS_2.

3.2. Seismic risk of pile foundation

Figure 8 shows seismic risk surfaces of piles at different limit states for different corrosion and scour scenarios. A quick view of both limit states indicates that an older bridge with a larger scour depth has a higher seismic risk. More specifically, regarding the role of scour depth, a comparison of two limit states shows that for LS_1, the examined scour depths have noticeable influence since the intact status (i.e., service time of 0 year), whereas for LS_2, such influence takes place until a service time of 40 years, and becomes more influential at the service time of 60 years, and finally tends to be ineffective at the service time of 80 years. Therefore, it can be concluded that the role of scour depth becomes significant during service time from 20 to 60 years in general.

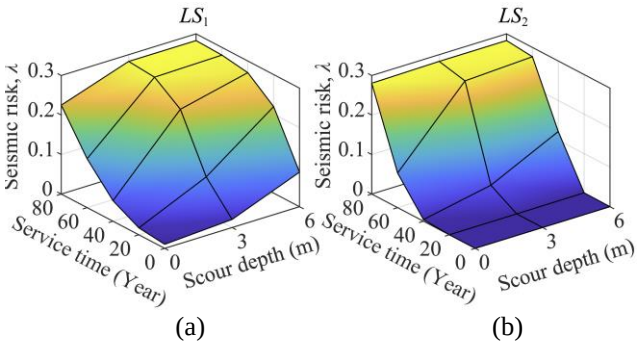

(a) (b)

Figure 8. Pile seismic risk at different limit states: (a) LS_1, and (b) LS_2.

4. CONCLUSIONS

This study investigates the lifetime seismic risk of coastal highway bridges against corrosion, scour and liquefaction effects. Three scour scenarios represented by scour depths of 0, 3, and 6 m, and five corrosion scenarios namely 0, 20, 40, 60, and 80 year(s) are examined. The following concluding remarks can be addressed:

(1) Service time of a bridge strongly affects the steel and concrete cover strengths. In particular, a 40 years service time leads to almost 50% degradation of stirrup strength, while for concrete cover, this level of degradation only needs 20 years.

(2) Seismic damage probabilities of the assessed bridge pile foundation increase with the increasing service time, regardless of scour depths and limit states.

(3) The role of scour depth becomes significant during the service time from 20 to 60 years.

The above findings can serve as preliminary references for risk-informed decision-making on management such as seismic retrofits of aging bridges subjected to scour and liquefaction threats.

5. ACKNOWLEDGMENT

This study is partially supported by the National Natural Science Foundation of China (52008155), USDOT TriDurLE project, and the Fundamental Research Funds for the Central Universities.

6. REFERENCES

Baker, J. W., Lin, T., Shahi, S. K., & Jayaram, N. (2011). *New ground motion selection procedures and selected motions for the PEER transportation research program*. Pacific Earthquake Engineering Research Center.

Capé, M. (1999). Residual service-life assessment of existing R/C structures. Chalmers University of Technology & Milan University of Technology.

Cornell, C. A., Jalayer, F., Hamburger, R. O., & Foutch, D. A. (2002). Probabilistic basis for 2000 SAC federal emergency management agency steel moment frame guidelines. *Journal of Structural Engineering*, *128*(4), 526–533.

Coronelli, D., & Gambarova, P. (2004). Structural assessment of corroded reinforced concrete beams: Modeling guidelines. *Journal of Structural Engineering*, *130*(8), 1214–1224.

Du, Y. G., Clark, L. A., & Chan, A. H. C. (2005). Residual capacity of corroded reinforcing bars. *Magazine of Concrete Research*, *57*(3), 135–147.

Gehl, P., Douglas, J., & Seyedi, D. M. (2015). Influence of the number of dynamic analyses on the accuracy of structural response estimates. *Earthquake Spectra*, *31*(1), 97–113.

Ghosh, J., & Padgett, J. E. (2010). Aging considerations in the development of time-dependent seismic fragility curves. *Journal of Structural Engineering*, *136*(12), 1497–1511.

Han, R., Li, Y., & van de Lindt, J. (2014). Seismic risk of base isolated non-ductile reinforced concrete buildings considering uncertainties and mainshock–aftershock sequences. *Structural Safety*, *50*, 39–56.

Lee, H.-S., & Cho, Y.-S. (2009). Evaluation of the mechanical properties of steel reinforcement embedded in concrete specimen as a function of the degree of reinforcement corrosion. *International Journal of Fracture*, *157*(1–2), 81–88.

Molina, F. J., Alonso, C., & Andrade, C. (1993). Cover cracking as a function of rebar corrosion: Part 2—Numerical model. *Materials and Structures*, *26*(9), 532–548.

Petersen, M. D., Moschetti, M. P., Powers, P. M., Mueller, C. S., Haller, K. M., Frankel, A. D., Zeng, Y., Rezaeian, S., Harmsen, S. C., Boyd, O. S., Field, N., Chen, R., Rukstales, K. S., Luco, N., Wheeler, R. L., Williams, R. A., & Olsen, A. H. (2015). The 2014 United States national seismic hazard model. *Earthquake Spectra*, *31*(S1), S1–S30.

Stewart, M. G., & Rosowsky, D. V. (1998). Structural safety and serviceability of concrete bridges subject to corrosion. *Journal of Infrastructure Systems*, *4*(4), 146–155.

Vu, K. A. T., & Stewart, M. G. (2000). Structural reliability of concrete bridges including improved chloride-induced corrosion models. *Structural Safety*, *22*(4), 313–333.

Wang, X., Ji, B., & Ye, A. (2020a). Seismic behavior of pile-group-supported bridges in liquefiable soils with crusts subjected to potential scour: Insights from shake-table tests. *Journal of Geotechnical and Geoenvironmental Engineering*, *146*(5), 04020030.

Wang, X., Luo, F., Su, Z., & Ye, A. (2017). Efficient finite-element model for seismic response estimation of piles and soils in liquefied and laterally spreading ground considering shear localization. *International Journal of Geomechanics*, *17*(6), 06016039.

Wang, X., Pang, Y., & Ye, A. (2020b). Probabilistic seismic response analysis of coastal highway bridges under scour and liquefaction conditions: does the hydrodynamic effect matter? *Advances in Bridge Engineering*, *1*(1), 19.

Wang, X., Shafieezadeh, A., & Ye, A. (2018). Optimal intensity measures for probabilistic seismic demand modeling of extended pile-shaft-supported bridges in liquefied and laterally spreading ground. *Bulletin of Earthquake Engineering*, *16*(1), 229–257.

Wang, X., Ye, A., & Ji, B. (2019). Fragility-based sensitivity analysis on the seismic performance of pile-group-supported bridges in liquefiable ground undergoing scour potentials. *Engineering Structures*, *198*, 109427.